JJMIE

Volume 5, Number 6, Dec. 2011
ISSN 1995-6665
Pages 495 - 507

Jordan Journal of Mechanical and Industrial Engineering

Four-Port Noise Model for the Diesel Particulate Filters (DPF)

Sayel M. Fayyad[a], Mohammad N. Hamdan*[,b], Suleiman Abu-Ein[a]

[a]Al-Balqa Applied University, Mechanical Engineering Department, Jordan
[b]University Cincinnati, School of Aerospace and Mechanical Engineering , USA

Abstract

This work presents a 2-D field model for the study of sound propagation in a diesel particulate filter (DPF) unit. The 2-D model is formulated using Navier-stocks, energy, and continuity equations in which the normal as well as transverse component of gas velocity are retained. Temperature, pressure, density, and velocities variations with time are assumed to be harmonic. By substituting these quantities in the governing Navier-stock, energy, and continuity equations, a set of 2-D partial differential equations with respect to space are obtained . The obtained 2-D partial differential equations are solved using an approximate Fourier series expansions. The main outcome of this approximate analytical study is a 2-D acoustic model for the exhaust gases emission, with the existence of the diesel particulate filter. The approximate 2-D model is used in this work for calculating values of wave propagation constant which includes both attenuation and phase shift, finding the acoustics impedance of the DPF unit, comparing between different types of the DPF based on sound transmission losses, soot loading and on noise and vibration damping characteristics, in addition to calculating the noise reduction factor (NRF). The obtained results are compared with those presented by other investigators and a good agreement and improvements can be noticed for the presented study.

1. Introduction

One of the leading technologies for meeting future particulate matter (PM) emission standards is the diesel particulate filter (DPF). These devices generally consist of a wall-flow type filter positioned in the exhaust stream of a diesel vehicle. As the exhaust gases pass through the system, particulate emissions are collected and stored. Because the volume of diesel particulates collected by the system will eventually fill up and even plug the filter, a method for controlling trapped particulate matter and regenerating the filter is needed. Diesel particulate filter is a superior system in the reduction of particulate matters because it can lead to a reduction of about 70% of the PM. It contains a large numbers of thin tubes or cavities with a diameter of about (1-2 mm), and (0.15-0.5 cm) length.

There are many types of DPF's such as: electric heater type, burner type (ceramic filter), and fuel additive type; the latter type is a honey-comb ceramic. The honey-comb type constitutes an additive supply and an electronic system. In this type Fe is used as an additive whereby iron oxide is formed which reacts with carbon and then it is converted to iron. The DPF is connected on the exhaust pipe, hence noise and vibration characteristics of exhaust system are changed and consequently affect the performance of the engine by developing back pressure, change temperature and velocity of the exhaust gases...etc. Hence building an acoustic model for the DPF is necessary for the assessment of the diesel engine performance.

The performance of a DPF has been the subject of many theoretical and experimental studies over the last two decades, e.g. [1-13]. Greevesm [2] studied the origin of hydrocarbons emission from diesel engines and he found that DPF can eliminate some of PM and it is very promising as an after-treatment technique. Yu and Shahed [3] studied the effects of injection timing and exhaust gas recirculation on emissions from a diesel engine and they classified DPF as filtration and regenerative technique.

Konstandopoulous et al. [4] studied the wall-flow diesel particulate filters pressure drop and coolant efficiency and described the coupling between neighboring channels using Daracy's law to model flow through a porous medium. Peal [5] made an approximation to the effect of mean flow on sound propagation in capillary tubes. Astley and Cumings [6] presented FEM solutions, based on simplified equations for waves in a visco-thermal fluid, for the problem of sound propagation in capillary tubes. They made analysis for the laminar flow with a parabolic velocity distribution and a quadratic cross-section. The simplification of the governing equations is based on that the axial gradients are much smaller than the gradients over the cross-section.

Dokumaci [7] using the same set of simplified equations showed that for the case of a plug flow and a circular cross-section an exact solution is possible. Using this model the acoustic two-port for a catalytic converter unit was derived. Ih et al. [8] developed an analytical solutions for sound propagation in capillary cylindrical tubes with a parabolic mean flow, by neglecting the radial component of the particle velocity. Jeong and Ih [9] showed by numerical solutions of the governing equations,

* Corresponding author. e-mail: mnader@ju.edu.jo

that including the radial particle velocity has a small but noticeable effect. Dokumaci [10,11] extended his earlier work to the case of rectangular narrow tubes with a plug flow. He used a solution procedure based on a weak (Galerkin) formulation, where the fields over the channel cross-section are expanded as double Fourier sinus series. Allam and Abom [12] studied the acoustic modeling and testing of DPF and considered it as an eigenvalue 1D problem. Allam and Abom [1] modified the 1D model using the classical (exact) Kirchhoff solution for a plane wave in a narrow tube. Their model is shown to be in close agreement with the predictions of the model presented in this work. Furthermore their model, which assumes isothermal sound propagation, works satisfactorily up to 800-1000 Hz for a typical filter at operating (hot) conditions. The above studies treated the ease of tubes with rigid and non-porous walls, which are not applicable for the case of DPF. In this work the model developed by Allam and Abom [1] as well as that developed in [13]are used and modified by taking into account the effect of transverse velocity.

2. Formulation and solution of the problem

The DPF will be divided, as in [1], into five parts, see Fig. 1 below. The inlet (IN), narrow pipes with impermeable walls (1) and (3), the ceramic section (2), and the outlet section (OUT). The DPF may be manufactured from different materials (Cordierite or Silicon Carbide for example) and in its most common form consists of a substrate of narrow channels in which each channel is blocked at one end. Adjacent channels have this blockage at alternate ends with this construction exhaust gas may enter at one end, but must pass through the wall of a channel before exiting and is thus termed a wall flow device. From this it is clear that the flow in y-direction can have a significant effect i.e. the transverse velocity may play a vital role and has an affect in by making the problem a 2-D one.

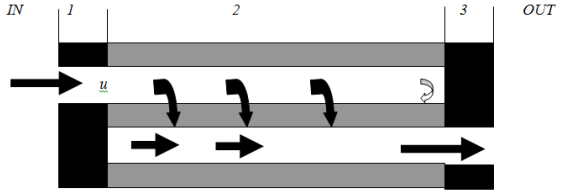

Figure (1) DPF sections and the 2D flow of gases.

2.1. Derivation of the Governing Equations:

The structure of diesel particulate filler (DPF) cells will be considered approximately square in the cross- section with a width about (1-2) mm. To develop an acoustic model for the sound propagation in the DPF unit after it is connected on the exhaust pipe, knowledge of the propagation constant for two – neighboring cells in the filter is required.

To derive the governing equations that describe the behavior of sound propagation in the filter and which may help in understanding of noise and vibration of the exhaust pipe after DPF unit is connected, the following simplifying assumptions are made :

- The DPF unit is considered completely as porous media.
- The transverse "normal" component of velocity (vyj) will not be neglected i.e. the model will be treated as a 2-D one.
- Flow in porous DPF unit is considered as viscous-thermal , incompressible, laminar, steady and Newtonian ideal gas flow.
- Chemical reactions are neglected.
- Pressure, temperature, velocities, and density are considered to vary harmonically with time.

To derive the governing equations the following basic forms of Navier – Stocks (momentum), continuity, energy and state equations are used.

Navier -Stocks equations:

$$\rho_{0j}\left[\frac{\partial u_{xj}}{\partial t}+u_{xj}\frac{\partial U_{0j}}{\partial x}+v_{yj}\frac{\partial U_{0j}}{\partial y}+w_{zj}\frac{\partial U_{0j}}{\partial z}\right]+\rho_{0j}U_{0j}\frac{\partial u_{xj}}{\partial x}= -\frac{\partial P_j}{\partial x}+\mu_j\left(\frac{\partial^2 u_{xj}}{\partial x^2}+\frac{\partial^2 u_{xj}}{\partial y^2}+\frac{\partial^2 u_{xj}}{\partial z^2}\right) \quad (1)$$

$$\rho_{0j}\left[\frac{\partial v_{yj}}{\partial t}+u_{xj}\frac{\partial V_{0j}}{\partial x}+v_{yj}\frac{\partial V_{0j}}{\partial y}+w_{zj}\frac{\partial V_{0j}}{\partial z}\right]+ \rho_{0j}V_{0j}\frac{\partial v_{yj}}{\partial y}=-\frac{\partial P_j}{\partial y}+\mu_j\left(\frac{\partial^2 v_{yj}}{\partial x^2}+\frac{\partial^2 v_{yj}}{\partial y^2}+\frac{\partial^2 v_{yj}}{\partial z^2}\right) \quad (2)$$

Continuity equation:

$$\frac{\partial \rho_j}{\partial t}+u_{xj}\frac{\partial \rho_{0j}}{\partial x}+U_{0J}\frac{\partial \rho_j}{\partial x}+\rho_j\frac{\partial U_{0j}}{\partial x}+\rho_{0j}\nabla.u_j=0 \quad (3)$$

Energy equation

$$\rho_{0j}Cp_j\left[\frac{\partial T_j}{\partial t}+U_{0j}\frac{\partial T_j}{\partial x}+u_{xj}\frac{\partial T_{0j}}{\partial x}\right]+\rho_j Cp_j U_{0j}\frac{\partial T_{0J}}{\partial x}= -\frac{\partial P_j}{\partial t}+U_{0j}\frac{\partial P_j}{\partial x}+\frac{\partial P_{0j}}{\partial x}u_{xj}+K_{thj}\nabla_s^2 T_j \quad (4)$$

State equation:

The gasses emission upon the exhaust pipe will be considered as an ideal gas so the state equation takes the form

$$\rho_j=\left(\frac{p_j}{R_J T_{0j}}\right)-\left(\frac{\rho_{0j}T_j}{T_{oj}}\right),\qquad \rho_j=\rho_j(x,y,z,t). \quad (5)$$

where

.

$$\rho_j=\rho_j(x,y,t)$$
$$T_j=T_j(x,y,z,t)$$
$$P_j=P_j(x,y,t) \quad (6)$$

x, y denotes the channel axis, u, v are the acoustic particle velocities, j = 1, 2 represent the inlet and outlet pipes, respectively, p, T and ρ are the acoustic pressure, temperature and density, respectively, μ is the shear viscosity coefficient, kth is the thermal conductivity of the fluid, R is the gas constant, Cp is the specific heat coefficient at constant pressure, P0, T0 and ρ0 denote the

ambient pressure, temperature and density, respectively, U0, V0 denotes the axial mean flow velocity and transverse velocity respectively, and denotes the Laplacian over the channel cross-section.

To describe the coupling between neighboring channels (which describes the porosity of diesel particulate filter) Darey's law is applied to the fluctuating fields:

$$p_1 - p_2 = R_w u_w \tag{8}$$

Where uw is the acoustic velocity through the wall and Rw is the wall resistance, which is given by Rw = μwht/σw, μw is the dynamic viscosity, ht is the wall thickness and σw is the wall permeability.

As indicated in the previous section, the problem will be treated as a 2D one, i.e.

$$\frac{\partial U_{0j}}{\partial z} = \frac{\partial^2 U_{0j}}{\partial z^2} = \frac{\partial V_{0j}}{\partial z^2} = \frac{\partial^2 V_{0j}}{\partial z^2} = 0 \tag{9}$$

At this stage u, v, P_j, ρ_j, T_j are considered to be varying with time only i.e. (time- harmonic variation) , that is

$$u_{xj} = A_0 e^{iwt}$$
$$v_j = B_0 e^{iwt} \tag{10}$$

$$\rho_j = \rho_0 e^{iwt},\ P_j = P_0 e^{-iwt},\ T_j = T_0 e^{iwt} \tag{11}$$

where $A_0, B_0, \rho_0, P_0, T_0$ are constant amplitudes. Substituting equation (9)-(11) into equations (1) to (4) one obtains:

$$\rho_{0j}\left[iw + U_{0j}\frac{\partial}{\partial x}\right]u_{xj} + \rho_{0j}\frac{\partial U_{0j}}{\partial x}u_{xj} + \rho_{0j}\frac{\partial U_{0j}}{\partial y}v_{yj} = -\frac{\partial P_j}{\partial x} + \mu_j\left(\frac{\partial^2 u_{xj}}{\partial x^2} + \frac{\partial^2 u_{xj}}{\partial y^2} + \frac{\partial^2 u_{xj}}{\partial z^2}\right) \tag{12}$$

$$\rho_{0j}\left[iw + V_{0j}\frac{\partial}{\partial y}\right]v_{yj} + \rho_{0j}\frac{\partial V_{0j}}{\partial y}v_{yj} + \rho_{0j}\frac{\partial V_{0j}}{\partial x}u_{xj} = -\frac{\partial P_j}{\partial y} + \mu_j\left(\frac{\partial^2 v_{yj}}{\partial x^2} + \frac{\partial^2 v_{yj}}{\partial y^2} + \frac{\partial^2 v_{yj}}{\partial z^2}\right) \tag{13}$$

$$\rho_{0j}Cp_j\left[iw + U_{0j}\frac{\partial}{\partial x}\right]T_j + \rho_j Cp_j\frac{\partial T_{0J}}{\partial x}u_{xj} + U_{0J}Cp_j\frac{\partial T_{0j}}{\partial x}\rho_j = (U_{0j}\frac{\partial}{\partial x} + iw)P_j + \frac{\partial P_{0j}}{\partial x}u_{xj} + K_{thj}\nabla_s^2 T_j \tag{14}$$

For verification if the problem is back treated as a 1D linear problem equations (12) -(14) will be shown later on to reduce to those given by Allam and Abom [1].

To get a full description to the acoustic model of the DPF unit, and then to find impedance, transmission losses, and other parameters used to assess the DPF unit performance, equations ((12) -(14) are solved analytically using the following approximations for the system variables:

$$\begin{aligned} P_j &= A_j \exp(-i\Gamma k_1 x),\\ u_{xj} &= H_j(x,y,z)P_j,\\ T_j &= F_j(x,y,z)P_j,\\ v_{yj} &= B_j \exp(-i\Gamma k_1 y) \end{aligned} \tag{15}$$

where Γ is a wave propagation constant.

Differentiating all terms in equation (15) and substituting them in equations (12) and (13) leads to

$$\begin{aligned} &\rho_{0j} iwH_j P_j + \rho_{0j} iU_{0j} H_j \Gamma k_1 P_j \\ &+ \rho_{0j}\frac{\partial U_{0j}}{\partial x}H_j P_j + \rho_{0j}\frac{\partial U_{0j}}{\partial y}H_j P_j \\ &= i\Gamma k_1 P_j + \mu_j\left(\frac{\partial^2 H_j}{\partial x^2} + \frac{\partial^2 H_j}{\partial y^2} + \frac{\partial^2 H_j}{\partial z^2}\right) \end{aligned} \tag{16}$$

Then dropping P_j and introducing the parameters

$$S_j^2 = \frac{\rho_{0j} w}{\mu_j} \quad , \quad M_j = \frac{U_{0j}}{C} \tag{17}$$

where S_j is the shear wave number, and M_j is Mach number, equation(16) becomes

$$\frac{\partial^2 H_j}{\partial x^2} + \frac{\partial^2 H_j}{\partial y^2} + \frac{\partial^2 H_j}{\partial z^2} - i(1 - \Gamma M_j + \frac{1}{iw}\frac{\partial U_{0j}}{\partial x} + \frac{\partial U_{0j}}{\partial y})S_j^2 H_j = \frac{-i\Gamma k_1}{\mu_j} \tag{18}$$

Next using the commonly employed definitions[1]

$$\beta_{xj}^2 = (1 - \Gamma M_{jx} + \frac{1}{iw}\frac{\partial U_{0j}}{\partial x} + \frac{\partial U_{0j}}{\partial y})S_j^2 \tag{19}$$

$$\beta_{yj}^2 = (1 - \Gamma M_{jy} + \frac{1}{iw}\frac{\partial V_{0j}}{\partial y} + \frac{\partial V_{0j}}{\partial x})S_j^2 \tag{20}$$

into equation (18), leads to

$$\frac{\partial^2 H_j}{\partial x^2} + \frac{\partial^2 H_j}{\partial y^2} + \frac{\partial^2 H_j}{\partial z^2} - i\beta_{xj}^2 H_j = \frac{-i\Gamma k_1}{\mu_j} \tag{21}$$

$$\frac{\partial^2 H_j}{\partial x^2} + \frac{\partial^2 H_j}{\partial y^2} + \frac{\partial^2 H_j}{\partial z^2} - i\beta_{yj}^2 H_j = \frac{-i\Gamma k_1}{\mu_j} \tag{22}$$

where $M_{jy} = \frac{V_0}{C}$ is the Mach number, and $k_1 = \frac{w}{C}$ is the wave number. Also substituting equation (15) in equation (14) one obtains

$$\rho_{0j}Cp_j iwF_j P_j - \rho_{0j}Cp_j iU_{0j}F_j\Gamma k_1 P_j + \rho_{0j}Cp_j \frac{\partial T_{0j}}{\partial x} H_j P_j + \rho_j Cp_j \frac{\partial T_{0j}}{\partial x} P_j = iw_1 P_j - iU_{0j}\Gamma k P_j \frac{\partial \rho_{0j}}{\partial x} H_j P_j + K_{thj}\left(\frac{\partial^2 F_j}{\partial x^2} + \frac{\partial^2 F_j}{\partial y^2} + \frac{\partial^2 F_j}{\partial z^2}\right)P_j \quad (23)$$

Next using state equation (5), rearranging and divided by P_j, and K_{thj} equation (23) yields

$$\frac{\partial^2 F_j}{\partial x^2} + \frac{\partial^2 F_j}{\partial y^2} + \frac{\partial^2 F_j}{\partial z^2} - \sigma_{jx}^2 F_j = \sigma_{0j}^2 + \sigma_{1j}^2 H_j \quad (24)$$

Where

$$\sigma_{jx}^2 = iS_j^2 \Pr(1 - \Gamma M_{jx} - \frac{U_{0j}}{iwT_{0j}}\frac{\partial T_{0j}}{\partial x}),$$
$$\sigma_{0jx}^2 = \frac{-iw}{K_{thj}}(1 + \frac{Cp_j U_{0j}}{iwR_j T_{0j}}\frac{\partial T_{0j}}{\partial x} - \Gamma M_{jx}),$$
$$\sigma_{1jx}^2 = \frac{1}{K_{thj}}(\rho_{0j}Cp_j \frac{\partial T_{0j}}{\partial x} - \frac{\partial P_{0j}}{\partial x}), \quad (25)$$
$$\Pr = \sqrt{\frac{\mu_J Cp_J}{K_{thj}}}$$

where Pr is the Prandtle number. In order to find a solution to equations (21) , (22) and (24) in a weak (Galerkian) sense, the fields *H*, and *F* are expanded in double Fourier Sine series [1] such that $H_{jx}(x, y, z)$ and *F* are assumed to be just varying in y and z directions only which implies that

$$\frac{\partial H_j}{\partial x} = 0, \quad \frac{\partial^2 H_j}{\partial x^2} = 0, \frac{\partial F_j}{\partial x} = 0, \frac{\partial^2 F_j}{\partial x^2} = 0 \quad (26)$$

And

$$H(0, y, z) = \sum_{m,n} a_{mn} \sin\frac{m\Pi y}{2a_j}\sin\frac{n\Pi z}{2a_j} \quad (27)$$

$$H(x, 0, z) = \sum_{\ln} a_{\ln} \sin\frac{l\Pi x}{2a_j}\sin\frac{n\Pi z}{2a_j} \quad (28)$$

where m, l, n=1, 3, 5, 7,…, and the expansion for *F* will be, for convenience, presented in a later part of this section. The above series includes only symmetric terms since the assumed pressure distribution is symmetric over the cross- section and the no slip wall boundary condition is assumed.

To calculate (a_{mn} *and* $a_{\ln}$)the above series are substituted into equation (21) the result is integrated over the cross-section and using the orthogonality property of the terms in these series one obtains ,

$$\sum_{m,n} a_{mn}\beta_j^2 \alpha_{mn}(\beta_j a_j) I_1 = \frac{-ik\Gamma_1}{\mu_j} I_2 \quad (29)$$

where

$$\alpha_{mn}(\beta_j a_j) = 1 + \frac{-\Pi^2}{4(\beta_j a_j)^2 (m^2 + n^2)} \quad (30)$$

$$I_1 = \iint_{a_j * a_j} \sin\frac{m\Pi y}{2a_j}\sin\frac{n\Pi z}{2a_j}\sin\frac{m'\Pi y}{2a_j}\sin\frac{n'\Pi z}{2a_j} dydz \quad (31)$$

$$I_2 = \iint_{a_j * a_j} \sin\frac{m'\Pi y}{2a_j}\sin\frac{n'\Pi z}{2a_j} dydz \quad (32)$$

Next carrying out the above integrations for m=m', n=n' and m ≠ m', n≠n', leads to

$$I_1 = \begin{cases} a_j^2, & m = m', n = n' \\ 0 & m \neq m' \\ 0 & n \neq n' \end{cases} \quad (33)$$

$$I_2 = \frac{16a_j^2}{m'n'\Pi^2} \quad (34)$$

where m, n and m', n' are odd integers= (1,3,5…..) . Substituting equations (33) and (34) into equation (29) gives

$$a_{mn}\beta_j^2 \alpha_{mn}(\beta_j a_j) a_j^2 = \frac{i\Gamma k_1}{\mu_j}\frac{16a_j^2}{mn\Pi^2} \quad (35)$$

Then solving the above equation for a_{mn} , one obtains

$$a_{mn} = \frac{16i\Gamma k_1}{mn\Pi^2 \beta_j^2 \alpha_{mn}(\beta_j a_j)\mu_j} \quad (36)$$

Also following the same procedure as above, using equation (22) instead of equation (21), leads to

$$a_{\ln} = \frac{16i\Gamma k_1}{mn\Pi^2 \beta_{jy}^2 \alpha_{mn}(\beta_{jy} a_j)\mu_j} \quad (37)$$

Similarly, an approximate solution to equation (24), and as indicated above, is obtained by using the approximations

$$F(x, y, z) = \sum_{mn} b_{mn} \sin\frac{m\Pi y}{2a_j}\sin\frac{n\Pi z}{2a_j} \quad (38)$$

$$F(x, y, z) = \sum_{\ln} b_{\ln} \sin\frac{l\Pi x}{2a_j}\sin\frac{n\Pi z}{2a_j} \quad (39)$$

Then following the same procedure used in calculating a_{mn}, $a_{ln,}$ yields

$$b_{mn} = \frac{-1}{\sigma_j^2 \alpha_{mn}(\sigma_j a_j)\mu_j}\left(\frac{16\sigma_{0j}^2}{\Pi^2 mn} + \sigma_{1j}^2 a_{mn}\right) \tag{40}$$

where b_{ln} are undefined and thus will be neglected, e.g, so the problem will be treated only in x- direction and the y-direction variations are ignored.

In order to get a complete solution for the acoustic problem, continuity equation (3) is solved as follows. First averaging equation (3) and sate equation (5) ,one has.

$$\begin{aligned}&(iw + U_{0j}\frac{\partial}{\partial x}) < \rho_j > + < u_{xj} > \frac{\partial \rho_{0j}}{\partial x} + \\ &U_{0J}\frac{\partial \rho_j}{\partial x} + < \rho_j > \frac{\partial U_{0j}}{\partial x} + < \rho_{0j}\nabla.u_j >= 0\end{aligned} \tag{41}$$

$$< \rho_j >= \frac{P_j}{R_j T_j}(1 - \rho_{0j} R_j < F_j >) \tag{42}$$

where

$$< f >= \frac{1}{4a_j^2}\iint_{2a_j * 2a_j} f dydz \tag{43}$$

$$< F_j >= \sum_{m,n}\frac{4b_{mn}}{mn\Pi^2} \tag{44}$$

$$\begin{aligned}&< u_{xj} >= P_j < H_j >, \text{ and} \\ &< H_j >= \sum_{m,n}\frac{4a_{mn}}{mn\Pi^2},\end{aligned} \tag{45}$$

To find $< \nabla.u_j >$, one writes

$$\begin{aligned}&< \nabla.u_j >= \frac{1}{4a_j^2}\iint_{2a_j * 2a_j}\left(\frac{\partial u_{xj}}{\partial x} + \frac{\partial v_{yj}}{\partial y} + \nabla_s.u_j\right)dydz = \\ &\frac{\partial < u_{xj} >}{\partial x} + \frac{\partial < v_{yj} >}{\partial y} + \frac{1}{4a_j^2}\oint_{c_j} u_j.n_j ds\end{aligned} \tag{46}$$

but

$$\oint_{c_j} u_j.n_j ds = (-1)^{j-1}\oint_{c_j}\bar{u}_w ds \tag{47}$$

and

$$\begin{aligned}&\frac{\partial < u_{xj} >}{\partial x} = -ik_1\Gamma P_j < H_j >, \text{and} \\ &\frac{\partial < v_{xj} >}{\partial y} = -ik_1\Gamma P_j < H_j >,\end{aligned} \tag{48}$$

where c_j is the curve around the channel perimeter and u_w is the acoustic wall velocity.
Then using Darcy's law (equation (7)).

$$\bar{u}_w = \frac{P - P_{21}}{R_w} \tag{49}$$

and substituting equations (48) and (49) into equation (47)gives:

$$\oint_{c_j} u_j.n_j ds = (-1)^{j-1}\frac{8a_j(P_1 - P_2)}{R_w} \tag{50}$$

Then substituting equations (48) and (50) into equation (41) yields

$$\begin{aligned}&(iw + U_{0j}\frac{\partial}{\partial x})(\frac{P_j}{R_j T_{0j}}(1 - \rho_{0j} R_J < F_J >) + \frac{\partial \rho_{0j}}{\partial x} P_j < H_j > \\ &+ \rho_{0j}(-2i\Gamma k_1 < H_J > P_j) + \frac{\partial U_{0j}}{\partial x}(\frac{P_j}{R_j T_{0j}}(1 - \rho_{0j} R_J < F_J >) \\ &+ < \rho_{0j}\nabla.u_j > + (-1)^{j-1}\frac{\rho_{0j} * 8a_j(P_1 - P_2)}{4a_j^2 R_w} = 0\end{aligned} \tag{51}$$

Rearrange equation (51) and substituting the value of P_j (given in equation (15)) one obtains

$$\begin{aligned}&\left[\begin{aligned}&\frac{1}{R_j T_{0j}}(iw - \Gamma k_1 U_{0J} + \frac{\partial U_{0j}}{\partial x})(1 - \rho_{0j} R_j < F_j >) \\ &+ (\frac{\partial \rho_{0j}}{\partial x} - 2ik_1\Gamma\rho_{0j}) < H_j >\end{aligned}\right] A_j + \\ &(-1)^{j-1} * \frac{2\rho_{0j}(A_1 - A_2)}{a_j R_w} = 0\end{aligned} \tag{52}$$

Then multiplying the above equation by ($\frac{R_w a_j}{2\rho_{0j}}$), leads to

$$\begin{aligned}&\left[\begin{aligned}&\frac{R_w a_j}{2\rho_{0j} R_j T_{0j}}(iw - \Gamma k_1 U_{0J} + \frac{\partial U_{0j}}{\partial x})(1 - \rho_{0j} R_j < F_j >) \\ &+ \frac{R_w a_j}{2\rho_{0j}}(\frac{\partial \rho_{0j}}{\partial x} - 2ik_1\Gamma\rho_{0j}) < H_j >\end{aligned}\right] A_j \\ &+ (-1)^{j-1}(A_1 - A_2) = 0\end{aligned} \tag{53}$$

The above equation represents a set of two linear homogeneous equations for the amplitudes of pressure waves A_1, A_2 in neighboring channels 1 and2 which can be written as [1]

$$\begin{bmatrix} K11 + K21 & -K12 \\ K21 & K12 - K22 \end{bmatrix}\begin{bmatrix} A_1 \\ A_2 \end{bmatrix} = \begin{bmatrix} 0 \\ 0 \end{bmatrix} \tag{54}$$

where

$$K_{1j} = \left[\begin{aligned}&\frac{R_w a_j}{2\rho_{0j} R_j T_{0j}}(iw - \Gamma k_1 U_{0J} + \frac{\partial U_{0j}}{\partial x})(1 - \rho_{0j} R_j < F_j >) + \\ &\frac{R_w a_j}{2\rho_{0j}}(\frac{\partial \rho_{0j}}{\partial x} - 2ik_1\Gamma\rho_{0j}) < H_j >\end{aligned}\right] \tag{55}$$

and

$$K_{2j} = (-1)^{j-1} \tag{56}$$

For a non trivial solution the determinant

$$\begin{vmatrix} K11+K21 & -K12 \\ K21 & K12-K22 \end{vmatrix} \quad (57)$$

is set equal to zero which leads to a transcendental equation for the propagation constant "Γ". By substituting numerical values of different constants and physical quantities, and by using "Matlab" for the case of no-mean flow i.e. (U_{0j}, V_{0j}=0) the obtained results for the values of the propagation constant are as follows.

For the case of cold conditions (T=293˚K,w=200-300 Hz):

Γ1=0.0005+0.0027i, Γ2=-0.0005-0.0023i,
Γ3= 0.0014+0.0008i, and Γ4=0.0014-0.0008i.

While for the specified hot conditions, (e.g, T=773˚K, w=400-1000 Hz), the obtained results are:

Γ1= $(0.2451+0.9873i)10^{-3}$, Γ2= $(-0.2451-0.9873i)10^{-3}$, Γ3= $(-0.7032+0.3440i)10^{-3}$, and Γ4= $(0.7032-0.3440i)10^{-3}$.

Plots and discussion of wave propagation constant variations with shear wave number are presented and discussed later on. Note that for each root of eigenvalues of Γ there is a corresponding 2-D mode (eigenvector) e_n. Using these eigenvectors and modes the general expression of these eigenvectors can be written as follows for the time harmonic variation.

$$\begin{pmatrix} \bar{p}_1(x) \\ \bar{p}_2(x) \end{pmatrix} = \sum_{n=1}^{4} \bar{a}_n e^{-ik_1\Gamma_n x} e_{,jn} \quad (58)$$

where $\bar{a}_n$ is the modal amplitude and $\bar{p}(x)$ is the acoustics pressure. For each acoustics pressure there is an acoustics volume velocity $\bar{q}_j(x)$ given by

$$\begin{pmatrix} \bar{q}_1(x) \\ \bar{q}_2(x) \end{pmatrix} = \sum_{n=1}^{4} \bar{a}_n e^{-ik_1\Gamma_n x} e^{'}_{,jn} \quad (59)$$

Where

$$e^{'}_{j,n} = 4a_j^2 < H_{j,n} > e_{j,n}$$

Then using equations (58) and (59) the total four port matrix can be written as:

$$\begin{pmatrix} \bar{p}_1(x) \\ \bar{p}_2(x) \\ \bar{q}_1(x) \\ \bar{q}_2(x) \end{pmatrix} = \begin{pmatrix} e^{-ik_1\Gamma_1 x}e_1 & e^{-ik_1\Gamma_2 x}e_2 & e^{-ik_1\Gamma_3 x}e_3 & e^{-ik_1\Gamma_4 x}e_4 \\ e^{ik_1\Gamma_1 x}e_1 & e^{ik_1\Gamma_2 x}e_2 & e^{ik_1\Gamma_3 x}e_3 & e^{ik_1\Gamma_4 x}e_4 \\ e^{-ik2\Gamma_1 x}e_1 & e^{-ik2\Gamma_2 x}e_2 & e^{-ik_2\Gamma_3 x}e_3 & e^{-ik_2\Gamma_4 x}e_4 \\ e^{ik_2\Gamma_1 x}e_1 & e^{ik_2\Gamma_2 x}e_2 & e^{ik_2\Gamma_4 x}e_3 & e^{ik_2\Gamma_4 x}e_4 \end{pmatrix} \begin{pmatrix} \bar{a}_1 \\ \bar{a}_2 \\ \bar{a}_3 \\ \bar{a}_4 \end{pmatrix} \quad (60)$$

where [1]

$$k_2 = k_1\sqrt{1-8i\beta/k_1} \quad \beta = C_j\rho_w/dh_jR_w <\text{Hj}> = 4a_{11}/\Pi^2 \quad (61)$$

Next applying boundary conditions at x=0, x=L, one has

$$\begin{pmatrix} \bar{p}_1(0) \\ \bar{p}_2(0) \\ \bar{q}_1(0) \\ \bar{q}_2(0) \end{pmatrix} = H(0) \begin{pmatrix} \bar{a}_1 \\ \bar{a}_2 \\ \bar{a}_3 \\ \bar{a}_4 \end{pmatrix} \quad (62)$$

and

$$\begin{pmatrix} \bar{p}_1(L) \\ \bar{p}_2(L) \\ \bar{q}_1(L) \\ \bar{q}_2(L) \end{pmatrix} = H(L) \begin{pmatrix} \bar{a}_1 \\ \bar{a}_2 \\ \bar{a}_3 \\ \bar{a}_4 \end{pmatrix} \quad (63)$$

From equation (64) it can be shown that

$$\begin{pmatrix} \bar{a}_1 \\ \bar{a}_2 \\ \bar{a}_3 \\ \bar{a}_4 \end{pmatrix} = H^{-1}(L) \begin{pmatrix} \bar{p}_1(L) \\ \bar{p}_2(L) \\ \bar{q}_1(L) \\ \bar{q}_2(L) \end{pmatrix} \quad (64)$$

$$\begin{pmatrix} \bar{p}_1(0) \\ \bar{p}_2(0) \\ \bar{q}_1(0) \\ \bar{q}_2(0) \end{pmatrix} = H(0)\ H^{-1}(L) * \begin{pmatrix} \bar{p}(L)_1 \\ \bar{p}_2(L) \\ \bar{q}_3(L) \\ \bar{q}_4(L) \end{pmatrix} \quad (65)$$

Introducing the notation $H(0)\ H^{-1}(L)$=S, the four-port matrix S can be used to find the two-port matrix T_2 by using rigid wall boundary conditions in channel 1 and 2 i.e.

$$\bar{q}_2(0) = 0,\ \bar{q}_1(L) = 0,$$

and

$$\begin{pmatrix} \bar{p}_1(0) \\ \bar{p}_2(0) \\ \bar{q}_1(0) \\ \bar{q}_2(0) \end{pmatrix} = \begin{pmatrix} S11 & S12 & S13 & S14 \\ S21 & S22 & S23 & S24 \\ S31 & S32 & S33 & S34_4 \\ S41 & S42 & S43 & S44 \end{pmatrix} \begin{pmatrix} \bar{p}(L)_1 \\ \bar{p}_2(L) \\ \bar{q}_3(L) \\ \bar{q}_4(L) \end{pmatrix} \quad (66)$$

which yields

$$\begin{aligned} \bar{p}_1(0) &= S11\left(\frac{-S44\bar{q}_2(L) - S42\bar{p}_2(L)}{S41}\right) + S12\bar{p}_2(L) + S14\bar{q}_2(L) \\ &= (S12 - S11S42/S41)\bar{p}_2(L) + (S14 - S11S44/S41)\bar{q}_2(L) \end{aligned} \quad (67)$$

and

$$\begin{aligned} \bar{q}_1(0) &= S31\left(\frac{-S44\bar{q}_2(L) - S42\bar{p}_2(L)}{S41}\right) + S32\bar{p}_2(L) \\ &= (S32 - S31S42/S41)\bar{p}_2(L) + (S34 - S31S44/S41)\bar{q}_2(L) \end{aligned} \quad (68)$$

Thus the two-port matrix can be written as

$$\begin{pmatrix} \bar{p}_1(x) \\ \bar{q}_2(x) \end{pmatrix} = T_2 \begin{pmatrix} \bar{p}_2(L) \\ \bar{q}_2(L) \end{pmatrix} \quad (69)$$

Where

$$T_2 = \begin{pmatrix} T11 & T12 \\ T21 & T22 \end{pmatrix}$$

If the number of channels at inlet (x=0) and outlet (x=L) is N then the total volume flow in all the open channels should be added, such that

$$T_2 = \begin{pmatrix} T11 & T12/N \\ NT21 & T22 \end{pmatrix} \quad (70)$$

where

$$\begin{aligned} T11 &= S12 - S42\,S11/S41 \\ T12 &= S14 - S44\,S11/S41 \\ T21 &= S32 - S42\,S31/S41 \\ T22 &= S34 - S44\,S31/S41 \end{aligned} \quad (71)$$

Substituting values of from above obtained results leads to the following expressions for the S matrix:

S_{COLD}= 1*e^3

$$\begin{pmatrix} 2.2079+0.3830i & -1.4236-0.1530i & -3.6978-0.9379i & -2.3229-0.7576i \\ 2.2079+0.3830i & -1.4236-0.1530i & -3.6978-0.9379i & -2.3229-0.7576i \\ (0.0009-0.0000i & -0.0005+0.0008i & 0.0003+0.0001i & 0.0002+0.0001i)*10\text{^-}2 \\ (-0.0009+0.0000i & 0.0005-0.0008i & -0.0003-0.0001i & -0.0002-0.0001i)*10\text{^-}2 \end{pmatrix} \quad (72)$$

S_{HOT}= 1*e^2

$$\begin{pmatrix} 9.4804+6.0904i & -5.9253-3.8065i & 3.4061-7.1114i & -2.6799-9.8755i \\ 9.4804+6.0904i & -5.9253-3.8065i & 3.4061-7.1114i & -2.6799-9.8755i \\ (-0.0012+0.0045i & 0.0011+0.0033i & 0.0064+.0002i & 0.0039-0.0001i)*10\text{^-}2 \\ (0.0012-0.0045i & -0.0011-0.0033i & -0.0064-.0002i & -0.0039+0.0001i)*10\text{^-}2 \end{pmatrix} \quad (73)$$

To obtain the acoustic resistance of the DPF, it is assumed that the acoustic field acts as a quasi-stationary disturbance of the steady state pressure drop (ΔP) over the filter unit. This pressure drop is modeled using Darcy's law with a quadratic Forcheimer extension - equation

$$\Delta p = R_1 U + R_2 U^2 \quad (74)$$

By differentiating this equation with respect to U one obtains

$$\begin{aligned} \frac{d(\Delta P)}{dU} &= \left(\frac{R_1 + 2R_2U}{A_f}\right) * A_f \\ d(\Delta P) &= \left(\frac{R_1 + 2R_2U}{A_f}\right) * A_f\, dU \end{aligned} \quad (75)$$

But since $dQ=A_f*dU$, one has

$$d(\Delta P) = R_{ac} dQ \quad (76)$$

Where

$$R_{ac} = \frac{R_1 + 2R_2U}{A_f} \quad (77)$$

R_{ac} is the acoustics resistance, and A_f is the filter cross-sectional area.

The above lumped impedance model can be used for the inlet and outlet sections including the adjacent short pipes. This implies that (for a two-port model)

$$T_x = \begin{pmatrix} 1 & Z_x \\ 0 & 1 \end{pmatrix} \quad (78)$$

Where

x=IN+1, or 3+OUT sections of the DPF.

$$Z_x = r_x + \frac{i\rho_x w l_x}{d_{hj}^2} \quad (79)$$

(79)

r is the acoustic resistance of the filter section , L is the end correction length and

d_{hj} is the hydraulic radius [1].

Note that, as indicated in [1],

$$r_{1+IN} = r_{3+OUT} = \frac{R_2 U_0}{A} \quad (80)$$

where R_2 can be given as

$$R_2 = \begin{cases} \rho_{IN}(1-1/m_{IN})^2/4 \\ \rho_{OUT}(1-1/m_{OUT})^2/2 \end{cases} \quad (81)$$

and m_{IN}, m_{OUT} are the open area ratios at inlet and outlet respectively. So by multiplying equation (81) by (C_j/C_j) and substitute equations (81) into equation (80) one obtains

$$Z_x = \begin{cases} Z_{IN} M_{IN}(1/m_{IN}^2 - 1) + \dfrac{i\rho w l_1}{d_{hj}^2 N} \\ 2Z_{OUT} M_{IOUT}(1-1/m_{OUT}) + \dfrac{i\rho w l_3}{d_{hj}^2 N} \end{cases} \quad (82)$$

Using equation (82) the full transforming matrices for different sections of the DPF can be written as follows

$$T_{IN} = \begin{pmatrix} 1/2 & Z_{IN} M_{IN}(1/m_{IN}^2 - 1) \\ 0 & 1/2 \end{pmatrix} \quad (83)$$

$$T_1 = \begin{pmatrix} 1/2 & \dfrac{i\rho w l_1}{d_{hj}^2 N} \\ 0 & 1/2 \end{pmatrix} \quad (84)$$

$$T_{OUT} = \begin{pmatrix} 1/2 & 2Z_{OUT} M_{OUT}(1-1/m_{OUT} \\ 0 & 1/2 \end{pmatrix} \quad (85)$$

$$T_3 = \begin{pmatrix} 1/2 & \dfrac{i\rho w l_3}{d_{hj}^2 N} \\ 0 & 1/2 \end{pmatrix} \quad (86)$$

Where

$$Z_{IN} = \frac{\rho_{IN} C_{IN}}{A_{IN}}, Z_{out} = \frac{\rho_{out} C_{outt}}{A_{out}} \quad (87)$$

Finally using the relations

$$T_{DPF} = T_{IN}\, T_1\, T_2\, T_3\, T_{out}, \quad (88)$$

$$TL = 20 \log |T_{DPF}/2| \quad (89)$$

Taking all terms of the matrix T_{DPF} in series and then applying equation (89) one obtains the transmission losses, which take the form

$$TL_{DPF} = 10\log_{10}\Big|\ (1/16)T_{11} + (1/8)iY_1NT_{21} + (1/8)NT_{21}Z_{IN}M_{IN}(1/m_{IN}^2 - 1) + (1/4)T_{11}Z_{OUT}M_{OUT}(1-1/m_{OUT}) + (1/2)iY_1NT21 + 0.5NT_{21}Z_{IN}M_{IN}(1/m_{IN}^2 - 1) + Z_{OUT}M_{OUT}(1-1/m_{OUT}) + (1/8)iY_3T_{11} - 0.25Y_3Y_1NT_{21} + 0.25iY_3NT_{21}Z_{IN}M_{IN}(1/m_{IN}^2 - 1) + (1/16)T_{12}NiY_3 - (1/8)Y_1Y_3T_{22} + (1/8)iY_3T_{22}Z_{IN}M_{IN}(1/m_{IN}^2 - 1) + (1/16)NT_{21} + 0.25NT_{21}Z_{OUT}M_{OUT}(1-1/m_{OUT}) + (1/8)NT_{21}iY_3 + (1/16)T_{22}\ \Big| \quad (90)$$

where *Y1* is the plug mass impedance of section 1 ($Y_1 = \frac{i\rho w l_1}{d_{hj}^2 N}$) and *Y3* is the plug mass impedance of section3 ($Y_3 = \frac{i\rho w l_3}{d_{hj}^2 N}$).

Note that the noise reduction factor can be calculated by using the following equation

$$NRF = LP_2 - LP_1 = 20\log\frac{P_2}{P_1} \quad (91)$$

Equation (90) will be used to find the values of transmission losses for different system parameters and for different types of DPF shown in Table (1).. The obtained results will be discussed in the next section .

3. Results and Discussion

3.1. Results:

For the case of time harmonic variation the attenuation are represented by the real parts of the propagation constant, as indicated in the previous section. Figure (2) represents the attenuation of the four real parts of the wave propagation constants for the cold conditions (293˚K. w=200-300Hz).

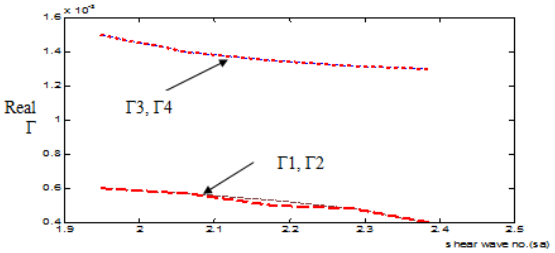

Figure 2: Real part of Γ vs. shear wave number (attenuation), ------ Γ1, ----- Γ2 propagation constants for uncoupled waves, …… Γ3,…… Γ4 propagation constants for coupled waves. (at cold conditions).

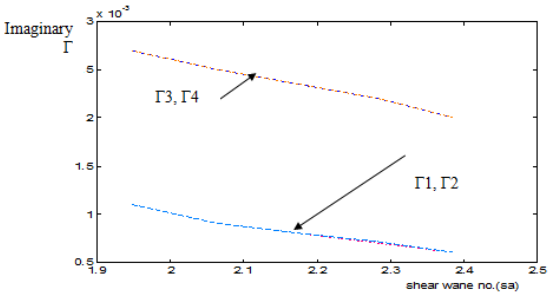

Figure 3: imaginary part of Γ vs. shear wave number (phase shift), ------ Γ1, ----- Γ2 propagation constants for uncoupled waves, …… Γ3,…… Γ4 propagation constants for coupled waves. (At cold conditions).

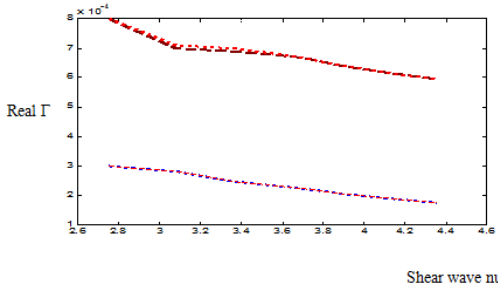

Figure 4: Real part of Γ vs. shear wave number (attenuation), ------ Γ1, ----- Γ2 propagation constants for uncoupled waves, ------- Γ3, ----- Γ4 propagation constants for coupled waves. (At hot conditions, T=773C, w=400-1000 Hz.).

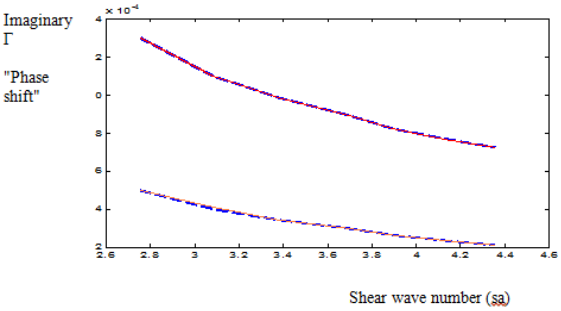

Figure 5: imaginary part of Γ vs. shear wave number (phase shift), ------ Γ1, ----- Γ2 propagation constants for uncoupled waves, …… Γ3,…… Γ4 propagation constants for coupled waves. (At hot conditions).

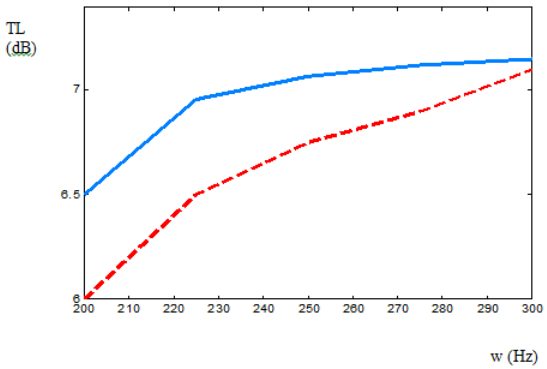

Figure 6: transmission losses vs. frequency in the case of cold conditions compared with last recent study [Allam], ----- red for Allam, while ____ blue is the proposed study, (With no soot layer) and Mach=0.02.

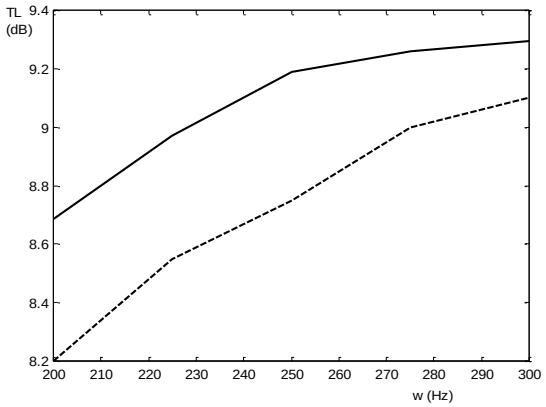

Figure 7: transmission losses vs. frequency in the case of cold conditions compared with last recent study [Allam], ----- for Allam, while _____ is for the proposed study, (With soot layer) and Mach=0.02.

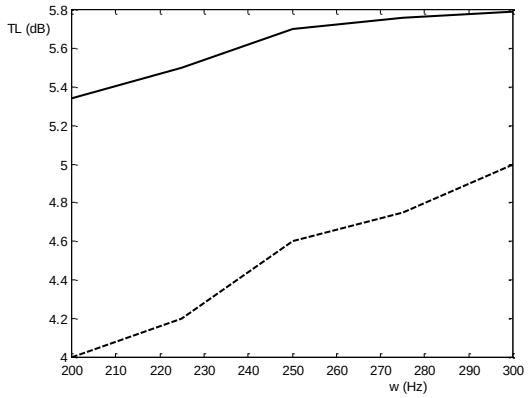

Figure 8: transmission losses vs. frequency for RC:200/12 DPF unit type in the case of cold conditions compared with last recent study [Allam], --- for Allam, while ___ is for the proposed study. (With no soot layer). Mach=0.02.

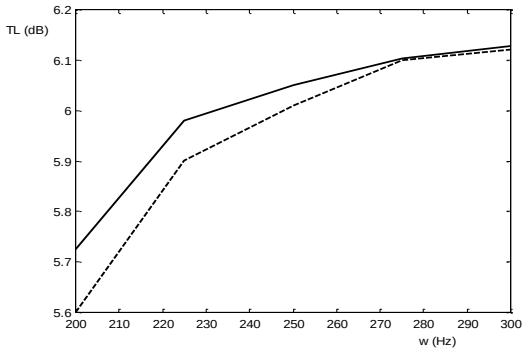

Figure 9: transmission losses vs. frequency for RC:200/20 DPF unit type in the case of cold conditions compared with last recent study [Allam], --- for Allam, while ____ is for the proposed study. (With no soot layer). Mach=0.02.

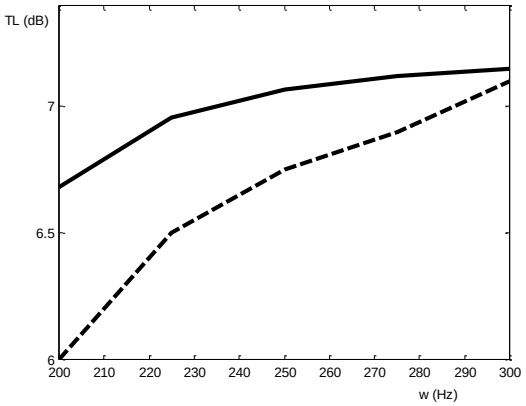

Figure 10: transmission losses vs. frequency for EX 80:200/14 DPF unit type in the case of cold conditions compared with last recent study [Allam], --- for Allam, while ____ for the proposed study. (With no soot layer). Mach=0.02.

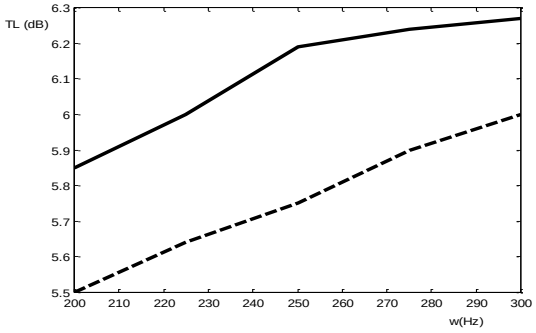

Figure 11: transmission losses vs. frequency for EX 80:100/17 DPF unit type in the case of cold conditions compared with last recent study [Allam], --- for Allam ____ is for the proposed study. (With no soot layer). Mach=0.02.

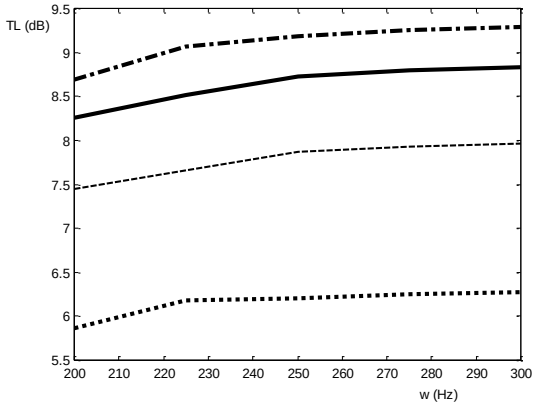

Figure 12: transmission losses vs. frequency, ___ for RC:200/12, -.-.-.for EX80:200/14, ……..for EX80:100/17, and----- for RC:200/20 DPF unit type in the case of cold conditions, (With soot layer). Mach=0.02.

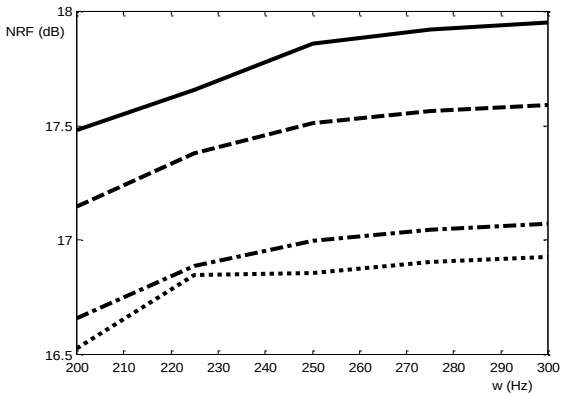

Figure 13: NRF vs. frequency, ------for RC: 200/12, ____ for EX80:200/14, -.-.-.-. for EX80:100/17, and……..for RC: 200/20 DPF unit type in the case of cold conditions, (With no soot layer). Mach=0.02.

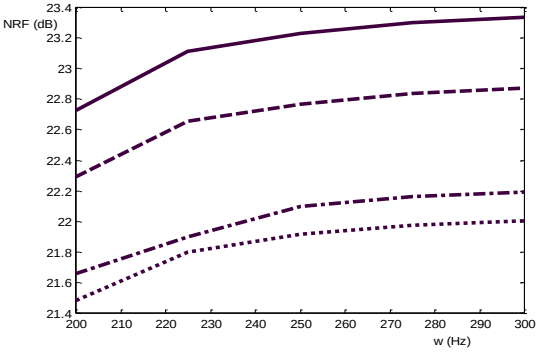

Figure 14: NRF vs. frequency, ------for RC: 200/12, ___ for EX80:200/14, -.-.-.-. for EX80:100/17, and……..for RC: 200/20 DPF unit type in the case of cold conditions, (With soot layer). Mach=0.02, cold conditions.

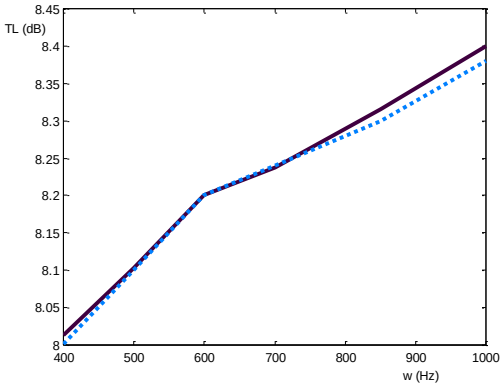

Figure 15: transmission losses vs. frequency in the case of hot conditions compared with last recent study [Allam], ----- for Allam, while ____ for the proposed study, (With no soot layer) and Mach=0.02.

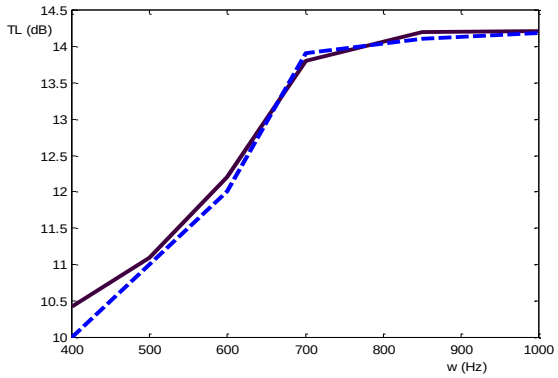

Figure 16: transmission losses vs. frequency in the case of hot conditions compared with last recent study [Allam], ----- for Allam, while ____ for the proposed study, (With soot layer) and Mach=0.02.

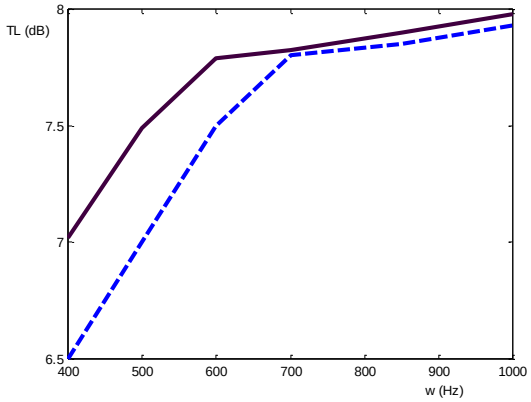

Figure 17: transmission losses vs. frequency for RC:200/12 DPF unit type in the case of hot conditions compared with last recent study [Allam], --- for Allam, while ____ is for the proposed study. (With no soot layer). Mach=0.02.

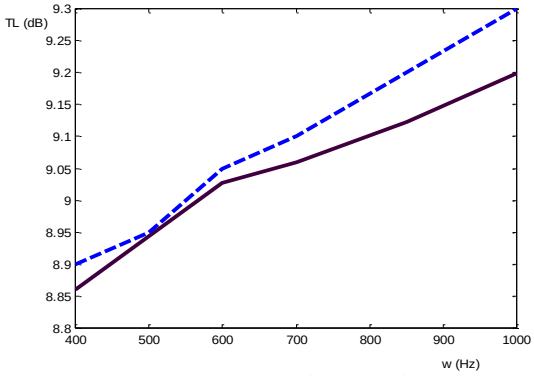

Figure 18: transmission losses vs. frequency for RC:200/20 DPF unit type in the case of hot conditions compared with last recent study [Allam], --- for Allam, while ___ is for the proposed study. (With no soot layer). Mach=0.02.

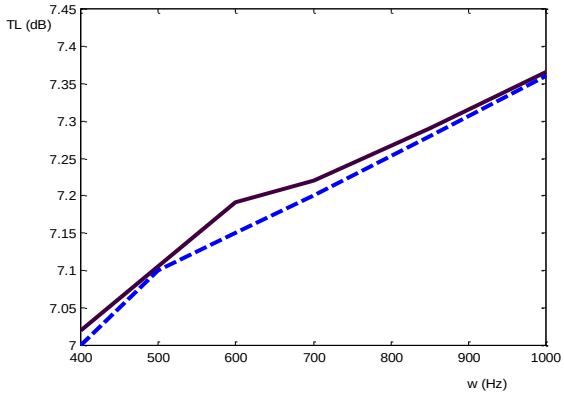

Figure 19: transmission losses vs. frequency for EX80:100/17 DPF unit type in the case of hot conditions compared with last recent study [Allam], ---for Allam ____ for the proposed study. (With no soot layer). Mach=0.02.

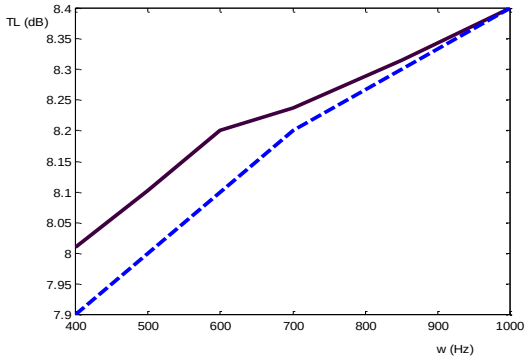

Figure 20: transmission losses vs. frequency for EX80:200/14 DPF unit type in the case of hot conditions compared with last recent study [Allam], ----for Allam, ____ is for the proposed study. (With no soot layer). Mach=0.02.

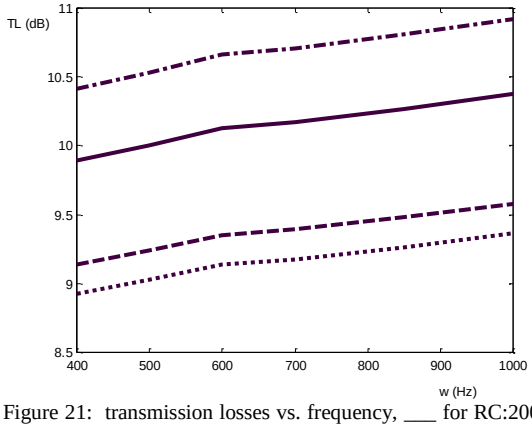

Figure 21: transmission losses vs. frequency, ___ for RC:200/12, -.-.-.for EX80:200/14, -----for EX80:100/17, and…..for RC:200/20 DPF unit type in the case of hot conditions, (With soot layer). Mach=0.02.

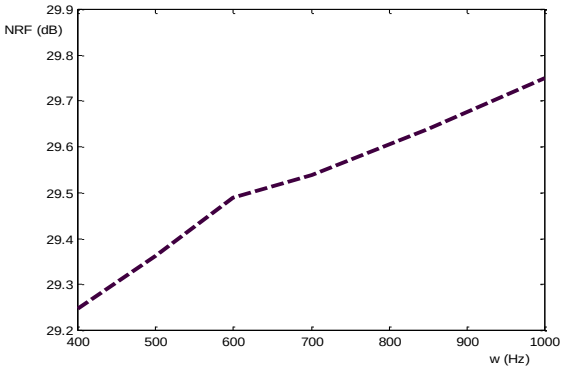

Figure 22: NRF vs. frequency for typical DPF in the case of hot conditions, (With soot layer). Mach=0.02.

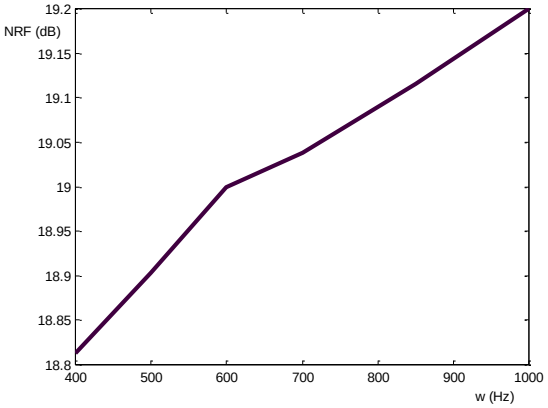

Figure 23: NRF vs. frequency for typical DPF in the case of hot conditions, (With no soot layer). Mach=0.02.

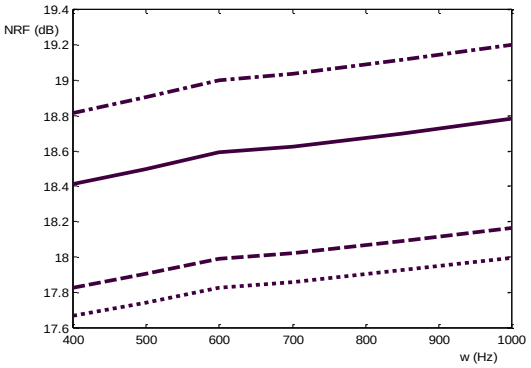

Figure 24: NRF vs. frequency, ___ for RC: 200/12, -.-.-. for EX80:200/14, -------for EX80:100/17, and…….for RC: 200/20 DPF unit type in the case of cold conditions, (With no soot layer). Mach=0.02.

  - Volume 5, Number 6 (ISSN 1995-6665)

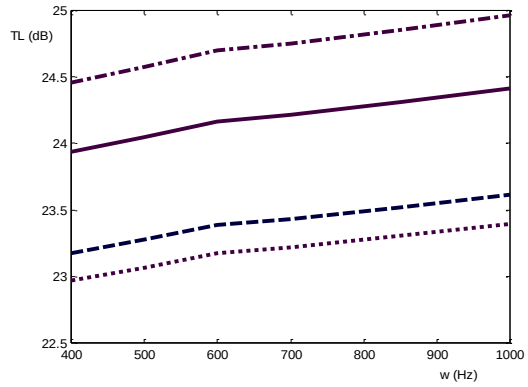

Figure 25: NRF vs. frequency, ____ for RC: 200/12, -.-.-. for EX80:200/14, -------for EX80:100/17, and……..for RC: 200/20 DPF unit type in the case of cold conditions, (With soot layer). Mach=0.02.

3.2. Discussion:

The propagation constants for a typical the diesel particulate filter (with specifications shown in table (1)), are shown in figures (2) to (5) for both cold and hot conditions for time harmonic variation. These roots can be divided into two parts: real and imaginary parts. The real parts , shown in figures (2), (4), represent the attenuation and correspond to uncoupled waves. While the imaginary parts of these roots represent the phase shift, figure (3), and (5). These parts correspond to coupled waves that are significantly more damped than the uncoupled waves. To investigate the predictions resulting from the proposed models and comparing them with the previous 1-D model by Allam [1] a typical DPF unit is analyzed. The results are plotted in two cases time harmonics variation (cold and hot). Figure (6) describes the transmission losses (TL) against the frequency in the case of time harmonic variation for the typical filter with no soot layer and for cold conditions. It can be noticed from figure (6) that the transmission losses are increased with frequency, by comparing TL of the proposed study with that of Allam [1] it can be noticed that there is an improvement in the proposed study, the more TL the more noise reduction. The reason that TL values for the proposed study are higher than that given by Allam [1] is that the proposed study deals with the flow of gases emission as a 2-D flow and so the flow in y-direction is not negligible as in last studies, hence TL can be of a noticeable value in y-direction. At w=300 Hz it can be noticed that there is a good agreement between two studies. Figure (7) describes TL for the typical filter with soot layer compared with Allam [1] at Mach =0.02. It can be noticed from the figure that there is a good agreement in the behavior but the TL for the proposed study is higher than that of Allam [1] (the dashed line), but a more agreement at higher frequency is achieved. Figures from (8) to (11) represent TL of different types of DPF unit with no soot layer, compared with results given by Allam [1], and it can be noticed from these figures that there is a good agreement in the behavior of TL against the frequency between the two studies, but there is an improvement for the proposed study. Figure (12) represents the TL of different types of DPF against frequency with soot layer, it can be noticed that EX80:200/14DPF type has the best capability of transmission losses, but EX80:100/17 DPF type has the lowest capability to do this. Figure (13) shows noise reduction factor (NRF) against frequency for different types of DPF unit, with no soot layer, it can be noticed that EX80:200/14 filter type has the best capability in noise reduction comparing with other types. In the same way figure (14) proves this but with soot layer. Figure (15) shows the TL versus frequency for the typical DPF unit in hot condition, time harmonic variation case compared with results given by Allam [10], with no soot layer, and M=0.02. From the figure a full agreement can be noticed between the proposed study and that given by Allam [1]. Also figure (16) shows TL versus frequency for the typical filter at hot conditions, time harmonic variation, M=0.02, and with soot layer. From last figure a good agreement between results given by last pervious study for Allam [1], and the proposed study. Figure (17) represents the relation between TL and frequency for RC: 200/12 DPF unit type at hot conditions, with no soot layer, M=0.02, and time harmonic variation. From last figure a good agreement between results given by last pervious study for Allam [1], and the proposed study. It can be noticed from last figure that the agreement between the proposed study and results of Allam is more at high frequencies. Figure (18) represents the relation between TL and frequency for RC: 200/20 DPF unit type at hot conditions, with no soot layer, M=0.02, and time harmonic variation. This figure shows a good agreement between results given by last pervious study for Allam [1], and the proposed study, but it can be noticed that TL values given by Allam for this type of DPF is higher than the proposed study. A full agreement between values of TL for EX80: 11/17 DPF unit type at the same previous conditions for the proposed study and values given by Allam [10] for the case of no soot layer can be seen in figure (19). Figure (20) represents the relation between TL and frequency for EX80: 200/14 DPF unit type at hot conditions, with no soot layer, M=0.02, and time harmonic variation. These figures show a good agreement between results given by Allam [1], and the present study specially at higher frequencies. Figure (21) represents transmission losses for different types of DPF unit, at hot conditions, time harmonic variation, M=0.02, and with soot layer. From lthe results in this figure it can be noticed that the EX80: 200/14 DPF unit type is the best one while RC: 200/20 DPF unit type is the worst. The variation of NRF with frequency for a typical filter at the same conditions is represented in figure (22) with soot layer and in figure (23) for no soot layer. The results in these two figures indicate that NRF with the existence of soot layer is more than that with no soot layer. An explanation for this behavior is that the soot layer forms a new absorber for noise but this is bad for gas emission reduction because the channels of the DPF unit becomes dirty and has less capability to make a reduction for gases emission. Figure (24) and figure (25) represent the relation between NRF and frequency (w), with no soot layer and with soot layer, respectively. From these two figures it can be noticed that EX80: 200/14 DPF unit type is the best type in noise reduction, while RC: 200/20 DPF unit type is the less efficient type in noise reduction operations.

3.3. Conclusion:

The main conclusions drawn from the results of this investigation can be summarized as follows:

- Wave propagation through the DPF unit leads to both attenuation and phase shift, and both attenuation and phase shift are damped as shear wave number increase.
- Both transmission loses and noise reduction factor for the typical filter and other types of DPFs tend to increase as frequency increases.
- Transmission losses for the case of existing soot layer are higher than those with no soot layer.
- EX80:200/14 DPF type has the best capability of transmission losses, but EX80:100/17 DPF type has the lowest capability to do this, and this appears in all cases and conditions.
- Transmission losses and NRF have a positive relationship with frequency.

Table 1: Filter Specifications.

1- Typical filter.

Diameter/length mm	channels/m^2 n x 10^{-5}	channels width mm	wall thickness mm	wall permeability
		d_h x 10^3m	ht x 10^4m	σ_w x 10^{13} m^2
150/250	3.10	1.44	3.55	2.5

2- Different types of filters.

Filter name	channels/m^2 n x 10^{-5}	channels width d_h x 10^3m	wall thickness ht x 10^4m	wall permeability σ_w x 10^{13} m^2	R1	R2
RC: 200/12	3.87	1.5	3.04	25	87.1	29.2
RC: 200/20	2.48	1.3	5.04	25	233.3	41.56
EX80: 100/17	1.55	2.11	4.3	2.5	199.8	30.92
EX80: 200/14	3.10	1.44	3.55	2.5	184.1	39.2

References

[1] S. Allam, S. M. Abom, "Sound propagation in an array of narrow porous channels with application to diesel particulate filters". Journal of Sound and Vibration, Vol. 291, 882-901, 2006.

[2] G. Greevesm, I. M. Khan, C. H. T. Wang, I. Fenne, "Origins of hydrocarbon emission from diesel engines". Society of Automotive Engineering, SAE Paper No. 770259, 1977, 02-01.

[3] R. Yu, Yu, S. M. Shahed, "Effects of injection timing and exhaust gas recirculation on emissions from a DI diesel engine". Society of Automotive Engineering, SAE Paper No. 811234, 1981.

[4] G. Konstandopoulos, J. H. Johnson, "Wall-flow diesel particulate filters - their pressure drop and collection efficiency", Society of Automotive Engineering, SAE Paper No. 890405, 1989.

[5] K. S. Peat, "A first approximation to the effects of mean flow on sound propagation in capillary tubes", Journal of Sound and Vibration Vol. 175, 1994, 475–489.

[6] R. J. Astley, A. Cummings, A., "Wave propagation in catalytic converter formulation of the problem and finite element scheme". Journal of Sound and vibration, Vol.188 , No. 5, 1995, 635–657.

[7] E. Dokumaci, "Sound transmission in narrow pipes with superimposed uniform mean flow and acoustic modeling of automobile catalytic converters", Journal of Sound and Vibration, Vol. 182 , 799–808, 1995.

[8] J.-G Ih, C. M. Park, H-J. Kim , " A model for sound propagation in capillary ducts with mean flow". Journal of Sound and Vibration Vol. 190, No.2, 163–175, 1996.

[9] K.-W. Joeng, J.-G. Ih, (1996). "A numerical study on the propagation of sound through capillary tubes with mean flow", Journal of Sound and Vibration, Vol. 198, No. 1, 67–79, 1996.

[10] E. Dokumaci, "On transmission of sound in circular and rectangular narrow pipes with superimposed mean flow". Journal of sound and vibration, Vol. 210, No. 3, 1998, 375–389,1998.

[11] E. Dokumaci, "An approximate dispersion equation for sound waves in a narrow pipe with ambient gradients". Journal of Sound and Vibration, Vol. 240, No. 4, 2001, 637–646.

[12] S. Allam, S. M. Abom, "Acoustic modeling and testing of diesel particulate filters ."Journal of Sound and Vibration, Vol. 288 (1/2) , 255–273, 2005.

[13] S. Fayyad, "Sound propagation in porous media with application to diesel" particulate filters." PhD Thesis, University of Jordan, 2006.